

Fluxional Characteristics of Palladium(II) Halide Complexes of Cyclic Selenoethers. A Dynamic Nuclear Magnetic Resonance Study

Edward W. Abel, Thomas E. MacKenzie, Keith G. Orrell, and Vladimir Šik
 Department of Chemistry, University of Exeter, Exeter EX4 4QD

The series of complexes $[\text{PdX}_2\{\overline{\text{Se}(\text{CH}_2)_n}\}_2]$ ($n = 4-6$; $X = \text{Cl, Br, or I}$) and $[\text{PdX}_2\{\overline{\text{SeCH}_2\text{CMe}_2\text{CH}_2}\}_2]$ ($X = \text{Cl, Br, or I}$) have been synthesised and their stereodynamics investigated by variable-temperature ^1H n.m.r. spectroscopy. Whereas conformational changes of the various sized ligand rings were always fast on the n.m.r. chemical shift time-scale, the rates of inversion of the co-ordinated selenium atoms were much slower and directly measurable by bandshape fitting methods. ΔG^\ddagger values for selenium inversion were in the range 66–78 kJ mol^{-1} . Values were observed to increase consistently with decreasing ligand ring size and are explained in terms of the extents of angle strain required to achieve the transition-state structure of the inversion process. The inversion energies of all four series of complexes reflect a *cis* halogen influence of 5.1–7.3 kJ mol^{-1} .

Co-ordination of Group 6 atoms sulphur and selenium to transition metals drastically increases the rates of pyramidal inversion of these atoms by a stabilisation of the transition-state structures primarily *via* ($p-d$) π conjugation and metal electronegativity effects.¹ This has enabled inversion dynamics of a wide range of S and Se complexes to be investigated by accurate dynamic n.m.r. methods.¹ Two earlier studies^{2,3} were concerned with the inversion characteristics of sulphur atoms incorporated in cyclic ligands which were complexed with palladium(II) and platinum(II) dihalides. We have now extended these studies to analogous selenium complexes in order to examine whether Se atomic inversion similarly is influenced by geometric factors such as ligand ring size and strain effects, and by electronic factors such as the nature of the metal and halogen.

Our original aim was to prepare the five series of complexes which are the selenium analogues of the earlier work on metal co-ordinated ring sulphides.² However, the three-membered complexes based on tetramethylselenirane could not be prepared as the ligand itself has only a transient lifetime⁴ and can only be isolated as a salt such as $[(\text{CH}_2)_2\overline{\text{SeC}_6\text{H}_4\text{Me-}p}][\text{SbF}_6]$.⁵ We therefore were restricted to preparing the complexes $[\text{PdX}_2\{\overline{\text{Se}(\text{CH}_2)_n}\}_2]$ ($n = 4-6$; $X = \text{Cl, Br, or I}$) and $[\text{PdX}_2\{\overline{\text{SeCH}_2\text{CMe}_2\text{CH}_2}\}_2]$ ($X = \text{Cl, Br, or I}$) (Figure 1). Complexes of 3,3-dimethylselenetane were prepared in preference to those of selenetane itself in order to minimise tendencies of the ligand and its complexes towards polymerisation in solution. We report the syntheses and variable-temperature ^1H n.m.r. studies on these complexes, many of which are new compounds.

Experimental

Ligands.—The ligands tetrahydroselenophene, $\overline{\text{Se}(\text{CH}_2)_4}$, and selenane, $\overline{\text{Se}(\text{CH}_2)_5}$, were synthesised by reported procedures.⁶⁻⁸ Selenepane, $\overline{\text{Se}(\text{CH}_2)_6}$, was prepared as follows. Sodium hydroxide (70 g, 1.75 mol), sodium hydroxymethanesulphinate, $\text{NaSO}_2\text{CH}_2\text{OH}$ (90 g, 0.75 mol), and selenium (25 g, 0.32 mol) were heated under reflux in water (350 cm^3). 1,6-Dibromohexane (78 g, 0.32 mol) was added slowly over a period of 30 min to the dark brown mixture, while continuing gentle reflux. The product was steam distilled as a milky-white pungent smelling liquid. After separation from co-condensed water the product was dried with anhydrous magnesium sulphate to give 5.5 g of crude product (yield 3.4%). No further

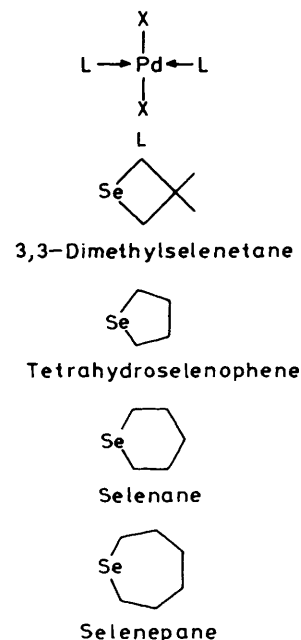


Figure 1. Selenoether complexes of palladium(II) dihalides ($X = \text{Cl, Br, or I}$)

distillation was carried out because of its tendency to polymerise.⁹

The preparative details for 3,3-dimethylselenetane given below are based on a literature procedure.¹⁰ Selenium powder (12.4 g, 0.16 mol) was added in portions to anhydrous liquid ammonia (600 cm^3) in a 1-dm³ three-necked flask. Potassium (13.4 g, 0.34 mol) was finely chopped and added in portions over 20 min until the solution remained blue. The ammonia was allowed to evaporate off overnight. The greyish white residue (K_2Se) was suspended in ethanol (400 cm^3 , 0 °C) and a solution of 1,3-dibromo-2,2-dimethylpropane (0.16 mol) in cold ethanol (100 cm^3) was added with stirring. The mixture was then heated under reflux for 6 h. After allowing to cool, the brown solution was filtered off from the grey-white residue and dissolved in 1.5 cm^3 of saturated NaCl solution. Organic products were extracted in diethyl ether (3 \times 150 cm^3), dried and distilled

Table 1. Characterisation of selenoether complexes of palladium(II) dihalides

Complex	Colour	M.p. (°C)	Analysis (%)			
			Found		Calc.	
			C	H	C	H
$trans-[PdCl_2\{SeCH_2CMe_2CH_2\}_2]$	Orange	136.7	24.2	4.15	25.3	4.25
$trans-[PdBr_2\{SeCH_2CMe_2CH_2\}_2]$	Brown	128*	21.0	3.35	21.3	3.6
$trans-[PdI_2\{SeCH_2CMe_2CH_2\}_2]$	Brown	117*	18.2	2.8	18.3	3.05
$trans-[PdCl_2\{Se(CH_2)_4\}_2]$	Yellow	190	20.5	3.65	21.45	3.6
$trans-[PdBr_2\{Se(CH_2)_4\}_2]$	Orange	186	17.3	3.0	17.9	3.0
$trans-[PdI_2\{Se(CH_2)_4\}_2]$	Dark brown	114	15.0	2.5	15.25	2.55
$trans-[PdCl_2\{Se(CH_2)_5\}_2]$	Orange	181	25.0	4.2	25.3	4.25
$trans-[PdBr_2\{Se(CH_2)_5\}_2]$	Brown	174	21.1	3.55	21.3	3.55
$trans-[PdI_2\{Se(CH_2)_5\}_2]$	Dark brown	147	18.1	3.25	18.2	3.05
$trans-[PdCl_2\{Se(CH_2)_6\}_2]$	Orange	160*	28.3	4.6	28.6	4.8
$trans-[PdBr_2\{Se(CH_2)_6\}_2]$	Brown	151*	23.7	4.05	24.3	4.1
$trans-[PdI_2\{Se(CH_2)_6\}_2]$	Brown-black	69*	20.7	3.3	21.2	3.55

* Decomposes.

giving several fractions, the one at 68 °C (12 mmHg, ca. 1600 Pa) proving to be the required product. Only 0.4 g of product was obtained and a large amount of unreacted selenium recovered.

Palladium(II) Complexes.—The general method of synthesis involved the action of the appropriate ligand on either an aqueous solution of $[PdX_4]^{2-}$ or a suspension of PdX_2 in chloroform. Preparative details of one complex from each of the four series will be given for exemplification. In all cases, crystals of the *trans* complexes were obtained (Table 1).

Dichlorobis(selenane)palladium(II). Potassium tetrachloropalladate(2-) (0.19 g, 0.58 mmol) was stirred in ethanol (20 cm³) in a Schlenk tube. Selenane (0.69 g, 46 mmol) in ethanol was added dropwise, immediately forming a yellow precipitate. After stirring for 2 h, the precipitate was filtered off from the pale yellow supernatant liquid and washed with hexane (2 × 5 cm³) and water (3 × 5 cm³). The product was then dried *in vacuo* prior to recrystallisation from hot acetone to give orange rod-like crystals of the desired complex $[PdCl_2\{Se(CH_2)_6\}_2]$ (93 mg, 0.20 mmol). Yield 34%.

Dibromobis(tetrahydro-selenophene)palladium(II). Potassium tetrabromopalladate(2-) (500 mg, 0.99 mmol) was dissolved in water (3 cm³) in a Schlenk tube. The brown solution was stirred whilst adding a solution of tetrahydro-selenophene (0.56 g, 3.9 mmol) in dichloromethane (4 cm³). A yellow-orange solid formed immediately, but after vigorous stirring for 2 h, the aqueous phase became almost colourless and the dichloromethane layer dark orange with some solid present. The organic phase was separated, taken to dryness, and the orange solid recrystallised from dichloromethane (20 cm³, 40 °C) and hexane (5 cm³) giving shiny orange-brown crystals of $[PdBr_2\{Se(CH_2)_4\}_2]$ (290 mg, 0.54 mmol). Yield 55%.

Di-iodobis(3,3-dimethylselenetane)palladium(II). Palladium di-iodide (66 mg, 0.18 mmol) was dissolved in potassium iodide (32 mg, 0.19 mmol) in water (5 cm³). The brown-red solution was treated with a solution of 3,3-dimethylselenetane (50 mg, 0.37 mmol) in ethanol (3 cm³). The solution immediately changed to a cloudy yellow suspension which on stirring for 4 h became brown. The mixture was pumped to dryness and the brown residue recrystallised from hot acetone and hexane to give brown crystals of $[PdI_2\{SeCH_2CMe_2CH_2\}_2]$ which were dried *in vacuo* (56 mg, 0.085 mmol). Yield 47%.

Dichlorobis(selenepane)palladium(II). A solution of selenepane (1.1 g, 6.0 mmol) in dichloromethane (10 cm³) was added to a stirred suspension of palladium dichloride (0.5 g, 2.82 mmol) in dichloromethane (20 cm³). The mixture was stirred overnight, and the dark orange-brown solid filtered off. The solid was extracted with hot dichloromethane (3 × 10 cm³) and the fractions combined and reduced in volume until precipitation occurred. The solution was then heated to boiling and allowed to cool, when red-brown crystals formed. The procedure was repeated to obtain a second crop of crystals of the desired complex $[PdCl_2\{Se(CH_2)_6\}_2]$. After drying *in vacuo* the total amount of product was 364 mg (0.72 mmol). Yield 26%.

Microanalyses.—These were carried out in this Department and at Butterworth Laboratories Ltd., London. Data are reported in Table 1.

Vibrational Spectra.—Infrared spectra of the complexes in n-hexane solution were recorded on a Perkin-Elmer model 299B spectrometer. Laser Raman and far-i.r. spectra were obtained at the Hungarian Institute of Isotopes, Budapest.

N.M.R. Spectra.—The majority of the 100-MHz ¹H spectra were recorded on a JEOL PFT-100 spectrometer operating in the Fourier-transform mode. The remaining spectra were obtained from a JEOL MH-100 continuous wave instrument. Temperature control was achieved with a standard JES-VT-3 unit calibrated with a copper-constantan thermocouple. Temperature measurements were made immediately prior to, and after, recording spectra.

Computations.—Our version of the DNMR3 program of Kleier and Binsch^{11a} was used for the n.m.r. bandshape analyses, matchings of experimental and computer synthesised spectra being done visually. A version of the LAOCNR program^{11b,c} was used when necessary for analysing low-temperature static spectra.

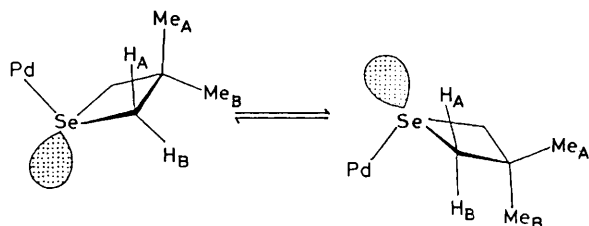
Results

All the 12 *trans*-palladium(II) dihalide complexes contain tetrahedral selenium atoms attached to prochiral alkane groups in which the geminal methylene protons are diastereotopic and

Table 2. Static n.m.r. data for $[\text{PdX}_2\{\text{SeCH}_2\text{CMe}_2\text{CH}_2\}_2]$ complexes*

X	$\delta(\text{H}_A)$	$\delta(\text{H}_B)$	J_{AB}/Hz	$\delta(\text{Me}_A)$	$\delta(\text{Me}_B)$
Cl	3.66	2.95	-10.3	1.53	1.30
Br	3.81	3.05	-10.9	1.51	1.31
I	4.06	3.18	-9.8	1.39	1.34

* In $\text{C}_6\text{D}_5\text{NO}_2$ solvent; chemical shifts in p.p.m. relative to SiMe_4 ($\delta = 0$ p.p.m.).

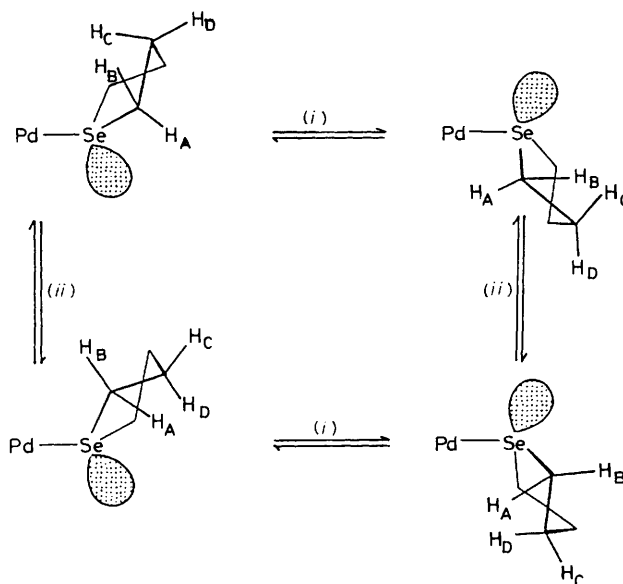
**Figure 2.** Selenium inversion in 3,3-dimethylselenetane complexes of palladium(II)

therefore anisochronous in the absence of any internal exchange process. Pyramidal inversion of the selenium atoms causes interchange of the anisochronous groups producing an exchange-averaged ^1H spectrum at high rates of inversion. In all cases, ring conformational changes (*e.g.* ring puckerings, pseudo-rotations, reversals, *etc.*) appeared to be fast on the n.m.r. time-scale and so pseudo-planar ring structures were assumed.

Four-membered Rings.—Attempts to prepare complexes of selenetane, $\text{Se}(\text{CH}_2)_3$, produced intractable polymers on heating. As it had been noted that oligomerisation of selenetane species proceeds *via* an initial loss of hydrogen from the 3-carbon of the ring,¹² 3,3-dimethylselenetane was prepared. Palladium(II) complexes of this ligand possessed greater solubility and solution stability compared to the unsubstituted ligand complexes and the variable-temperature ^1H spectra of all three dihalide complexes were studied without difficulty. The ground-state conformation of the selenetane ring deviates by only 24° from planarity,¹³ with a potential barrier of 3.4 kJ mol^{-1} separating the conformers. Conformational interconversion will therefore be fast on the n.m.r. time-scale and the ligand rings can be treated as effectively planar.

Selenium inversion causes the environments of the geminal protons and methyl groups to be interchanged as shown in Figure 2. The dynamic spin systems may be quite accurately described as $\text{AB} \rightleftharpoons \text{BA}$ and $\text{A}_3\text{B}_3 \rightleftharpoons \text{B}_3\text{A}_3$, since (i) no vicinal couplings were detected between the methylene and methyl protons, (ii) no four-bond couplings were observed between the ring methylene groups, and (iii) ^{77}Se satellite signals of the methylene absorptions were neglected.

Chemical shift and scalar coupling data are given in Table 2. Variable-temperature studies in the range ambient to 140°C produced the expected coalescences of the methylene and methyl signals. The methyl doublet coalesced at *ca.* 90°C and the methyl AB quartet at *ca.* 116°C . Both spectral regions were modelled by standard bandshape methods, the 'best fit' rate constants varying in the range $0.1\text{--}118 \text{ s}^{-1}$ for the methyl region and in the range $3.5\text{--}850 \text{ s}^{-1}$ for the methylene region. Arrhenius and Eyring energy parameters based on both sets of fittings were in good agreement.

**Figure 3.** Selenium inversion (i) and ring pseudo-rotation (ii) in tetrahydrosephenone complexes of palladium(II)

Five-membered Rings.—The three dihalide complexes gave similar $100\text{-MHz } ^1\text{H}$ spectra. In all cases, complexation caused high-frequency shifts compared to the free ligand, this effect being particularly pronounced for the α -methylene protons. The coupling patterns of the proton signals are complex as a result of the variety of geminal and vicinal scalar couplings occurring. At room temperature there is no evidence for more than one isomer of each complex, implying either a single fixed, ligand ring conformation or an equilibrium between several conformers which generates average proton environments. Far-i.r. and Raman spectra reveal the free ligand as an equilibrium structure of two low-energy half-chair conformations.¹⁴ Interconversion between these forms occurs by pseudo-rotation with a barrier of 22.5 kJ mol^{-1} . Assuming that there is no measurable interaction between the two ligand rings through the palladium atom, the interconversion of proton environments arising from both pseudo-rotation and selenium pyramidal inversion can be represented by Figure 3. At room temperature the ^1H spectra consist of only three absorption regions from which it is apparent that the ligand ring has an effective plane of symmetry. This clearly implies fast pseudo-rotation on the n.m.r. time-scale as expected from its magnitude of energy barrier. By the same measure, selenium inversion must be slow or absent as distinct signals are observed for the geminal protons on the α -ring carbons. Increasing the temperature leads to bandshape changes which are temperature reversible. These are clearly due to selenium inversion and the α -methylene region is most greatly affected. Bandshape analysis of the spectrum strictly requires computation of a dynamic spin problem of type $[\text{ABCD}]_2 \rightleftharpoons [\text{BADC}]_2$, where A,B refer to the α -methylene shifts and C,D to the β -methylene shifts. However, no four-bond couplings were detected and so analysis was based on a $\text{ABCD} \rightleftharpoons \text{BADC}$ system. This is valid if only the high frequency A,B regions are fitted. The β -methylene protons C,D experience coupling to *all* the other protons and so it was not possible to obtain a satisfactory fit of their signals. Exactly the same problem was encountered with the analogous sulphur complexes.² Analysis of the static spectrum using the LAOCNR program was based on the published analysis of the free ligand spectrum.¹⁵ The iterated chemical shifts and scalar coupling data are given in Table 3. Having obtained a satisfactory analysis of the AB

Table 3. Static n.m.r. data for $[\text{PdX}_2\{\text{Se}(\text{CH}_2)_n\}_2]$ ($n = 4$ or 5) complexes*

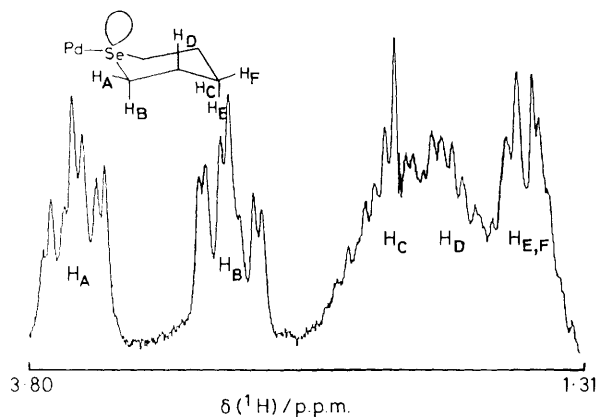
Complex	δ_A	δ_B	J_{AB}/Hz	J_{AC}/Hz	J_{AD}/Hz	J_{BC}/Hz	J_{BD}/Hz
$[\text{PdCl}_2\{\text{Se}(\text{CH}_2)_4\}_2]$	3.74	2.71	-11.0	6.8	6.1	6.9	7.1
$[\text{PdBr}_2\{\text{Se}(\text{CH}_2)_4\}_2]$	3.87	2.82	-10.9	6.8	6.3	6.3	6.5
$[\text{PdI}_2\{\text{Se}(\text{CH}_2)_4\}_2]$	4.02	3.02	-10.9	6.8	6.6	5.4	6.9
$[\text{PdCl}_2\{\text{Se}(\text{CH}_2)_5\}_2]$	3.20	2.43	-11.3	9.3	2.2	2.7	7.4
$[\text{PdBr}_2\{\text{Se}(\text{CH}_2)_5\}_2]$	3.30	2.70	-11.5	8.5	2.9	3.0	8.2
$[\text{PdI}_2\{\text{Se}(\text{CH}_2)_5\}_2]$	3.41	3.00	-11.6	8.4	3.0	3.1	8.3

* Solvent $\text{C}_6\text{D}_5\text{NO}_2$ - C_6D_6 ; all shifts in p.p.m. relative to SiMe_4 ($\delta = 0$ p.p.m.).

Table 4. The relationship between torsional barriers of X-C bonds and reversal energies of six-membered heterocyclic rings

CH_3ECH_3	$V_a/\text{kJ mol}^{-1}$	Ref.	$(\text{CH}_2)_5\text{E}$	$\Delta G^\ddagger/\text{kJ mol}^{-1}$	Ref.
$\text{CH}_3\text{CH}_2\text{CH}_3$	13.8	<i>a</i>	$(\text{CH}_2)_5\text{CH}_2$	43.1	<i>b</i>
CH_3OCH_3	10.5	<i>c</i>	$(\text{CH}_2)_5\text{O}$	43.1	16
CH_3SCH_3	8.9	<i>d</i>	$(\text{CH}_2)_5\text{S}$	39.5	16
CH_3SeCH_3	6.3	<i>e</i>	$(\text{CH}_2)_5\text{Se}$	34.5	16
CH_3TeCH_3	5.0	<i>f</i>	$(\text{CH}_2)_5\text{Te}$	30.5	16

^a W. D. Gwinn and K. S. Pitzer, *J. Chem. Phys.*, 1942, **10**, 428. ^b F. A. L. Anet, 'Dynamic Nuclear Magnetic Resonance Spectroscopy,' eds. L. M. Jackman and F. A. Cotton, Academic Press, New York and London, 1975, p. 579. ^c J. R. Durig and Y. S. Li, *J. Mol. Struct.*, 1972, **13**, 459. ^d M. Hayashi and L. Pierce, *J. Chem. Phys.*, 1961, **35**, 479. ^e J. F. Beecher, *J. Mol. Spectrosc.*, 1966, **21**, 414. ^f J. Bragin, J. R. Durig, Y. S. Li, and C. M. Player, *J. Chem. Phys.*, 1971, **55**, 2895.

**Figure 4.** Room-temperature 100-MHz ^1H spectrum of $[\text{PdCl}_2\{\text{Se}(\text{CH}_2)_5\}_2]$

portion of the ABCD system, total bandshape analysis of this portion of the four-spin system was carried out for the above-ambient temperature spectra. Close matchings of experimental and computer synthesised spectra were achieved in all cases.

Six-membered Rings.—Physical data for these complexes are given in Table 1. Far-i.r. and Raman studies on the complex $[\text{PdCl}_2\{\text{Se}(\text{CH}_2)_5\}_2]$ confirmed the centrosymmetric nature of a *trans* complex from the fact that bands were either i.r. active (*viz.* 343 cm^{-1} , Pd-Cl stretch; 238 cm^{-1} , Pd-Se stretch) or Raman active (*viz.* 295 cm^{-1} , Pd-Cl stretch; 164 cm^{-1} , Pd-Se stretch). Bending vibrations at lower wavenumbers were also observed but not assigned.

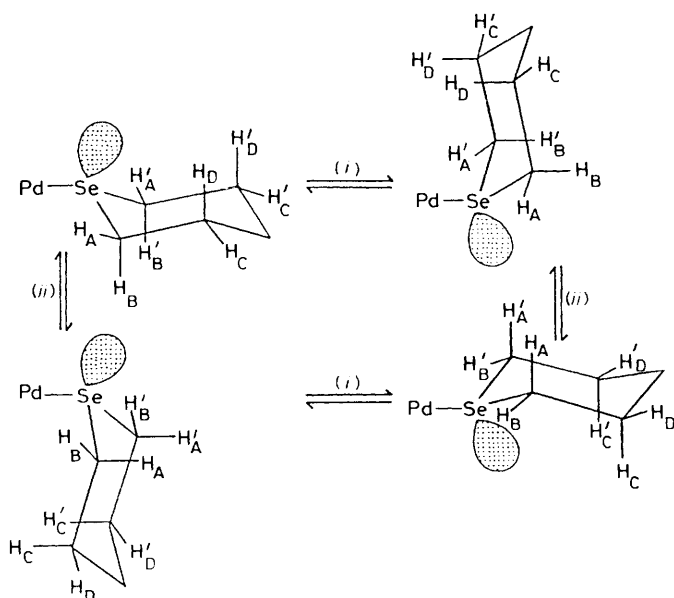
The room-temperature n.m.r. spectra of all three dihalide complexes show five absorption regions. The spectrum of the chloro-complex is illustrated in Figure 4. On raising the sample temperature, the two highest frequency absorption regions A,B and the central regions C,D exhibit clear coalescence features.

From experience with the pentamethylene sulphide complexes, these spectral changes are attributed to selenium atomic inversion. However, the dynamics of chair-to-chair ring reversal need to be considered. In the ring sulphide ligand complexes,^{2,3} the ring reversal process also contributed to the ^1H spectral lineshape changes at low temperatures. It has been shown previously¹⁶ that chair-to-chair ring reversal barriers depend primarily on torsional strain effects as represented by torsional barriers to rotation, V_a . Such barriers can be measured by far-i.r.-Raman methods and data for systems, CH_3ECH_3 ($\text{E} = \text{CH}_2, \text{O}, \text{S}, \text{Se}, \text{or Te}$), are given in Table 4 together with ring reversal energies for the appropriate pentamethylene chalcogen rings.¹⁶ It has been established³ that a transition metal only slightly influences the ring reversal transition state. Thus, the ΔG^\ddagger data in Table 4 are expected to be only slightly increased on complexation with palladium(II). These data therefore indicate that first the chair-to-chair reversal process in the dihalogenopalladium(II) complexes of selenane will be a substantially lower energy process than the selenium atom inversion process, and secondly that it will be of slightly lower energy than the corresponding process in the thiane complexes. For these reasons, the spectral changes observed in the range 20 – 140°C were attributed to varying rates of selenium inversion in the presence of rapid ring reversal which creates pseudo-planar six-membered rings. The full dynamic situation is indicated in Figure 5. Under this scheme the dynamic spin problem for selenium inversion is strictly described as an exchanging 10-spin problem. However, in the absence of four-bond scalar couplings and by restricting the band fittings to the α -methylene region, as was done in the five-membered ring systems, the spin problem may again be reduced to that of $\text{ABCD} \rightleftharpoons \text{BADC}$. Simulation of the AB portion was carried out using the LAOCNR iterative program and the best fit chemical shifts and scalar couplings given in Table 3. The vicinal couplings were assigned to the appropriate protons by considering the magnitudes of the dihedral angles relating different proton pairs, and then applying the Karplus equations.¹⁷ Although rapid ring reversal is operating, account

Table 5. Dihedral angles ($^{\circ}$) between vicinal protons in $[\text{PdX}_2\text{-}\{\text{E}(\text{CH}_2)_5\}_2]$ complexes

Vicinal pair*	Pd equatorial	Pd axial
H_AH_C	60	180
H_AH_D	60	60
H_BH_C	60	60
H_BH_D	180	60
H_CH_E	55	65
H_CH_F	65	175
H_DH_E	175	65
H_DH_F	65	55

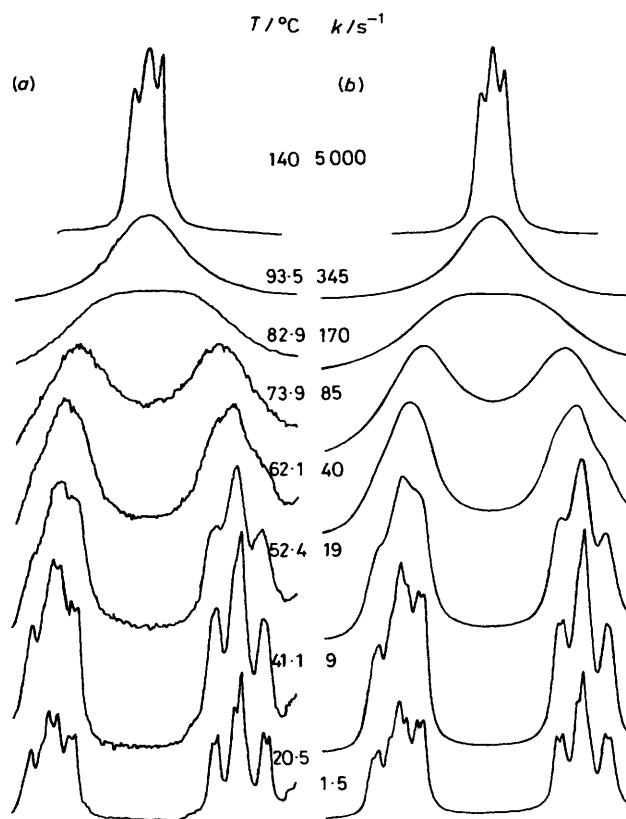
* Labelling refers to Pd equatorial structure (Figure 4). Ring reversal interchanges the geminal proton pairs H_A/H_B , H_C/H_D , and H_E/H_F .

**Figure 5.** Selenium inversion (i) and ring reversal (ii) in selenane complexes of palladium(II)

has to be taken of the likely unequal weighting of the static conformational structures (*i.e.* Pd axial and Pd equatorial). The calculated dihedral angles for the vicinal proton pairs are given in Table 5. As it was impossible to detect individual conformers even at the lowest temperatures (see later) it was assumed from the previous work^{2,3} that the equatorial conformers predominate but there is significant contribution (*e.g.* *ca.* 33%) from the axial forms. In such circumstances Table 5 indicates that $^3J_{AC} > ^3J_{AD}$ and $^3J_{BD} > ^3J_{BC}$ and this is the basis of the assignments in Table 3.

Bandshape fittings were performed on the A,B regions of the spectra in the temperature range 10–140 $^{\circ}\text{C}$. Good visual matchings were achieved at all temperatures, thus validating the simplification of the dynamic problem to that of a four-spin system. The experimental and computer simulated spectra of $[\text{PdCl}_2\{\text{Se}(\text{CH}_2)_5\}_2]$ are illustrated in Figure 6.

An attempt was made to study the conformational equilibria of the complexes by cooling solutions in $\text{CS}_2\text{-CD}_2\text{Cl}_2$ mixtures down to *ca.* -110°C . Although some broadening of the signals was apparent this could not be attributed conclusively to the retardation of chair-to-chair ring reversal. The use of fluorocarbon solvents (*e.g.* CF_2Cl_2) for extending the low-temperature range proved fruitless because of the negligible solubility of

**Figure 6.** Experimental (a) and computer synthesized (b) ^1H spectra of the α -methylene protons of $[\text{PdCl}_2\{\text{Se}(\text{CH}_2)_5\}_2]$ in the above-ambient temperature range

the complexes in these solvents. More conclusive evidence for ring reversal effects was obtained from a 63-MHz carbon-13 study of the dihalide complex. At room temperature the ^{13}C spectrum of this complex in $\text{CS}_2\text{-CD}_2\text{Cl}_2$ consists of three signals at δ 24.4, 24.6, and 25.6 in the intensity ratio 1:2:2. On cooling to the low-temperature limit of the solvent mixture (*ca.* -110°C) gross changes were observed in positions and line widths of the signals, but no analysis was possible. Nevertheless, the changes may be attributed with certainty to ring reversal effects coming within the ^{13}C n.m.r. time-scale.

Seven-membered Rings.—Physical data for the three selenepane complexes are given in Table 1. These complexes were somewhat more soluble in organic solvents than their smaller ring counterparts, probably as a result of the greater organic constitution of these complexes. Seven-membered alicyclic rings can exist in a variety of conformations, the twist-chair and twist-boat types being most favoured for cycloheptane.¹⁸ However, their interconversion follows low-energy pathways outside the scope of dynamic n.m.r. One implication of this ring flexibility is that the trigonal transition state associated with atomic inversion at selenium in selenepane rings is not expected to be raised in energy significantly by ring strain effects.

The room-temperature spectrum of the three complexes showed three main absorption regions of equal relative intensities centred at *ca.* δ 1.75, 2.1, and 3.3. The multiplet structures of all regions were complex and not fully resolved. The highest frequency region, due to the α -methylene protons, displays a distorted pseudo-triplet structure in the case of the iodo-complex. This implies that either selenium inversion is fast producing a time-averaged methylene proton shift or that

Table 6. Arrhenius and Eyring energy data* for Se inversion in selenoether complexes of palladium(II) dihalides

Complex	$E_a/\text{kJ mol}^{-1}$	$\log_{10}(A/s^{-1})$	$\Delta G^\ddagger/\text{kJ mol}^{-1}$	$\Delta H^\ddagger/\text{kJ mol}^{-1}$	$\Delta S^\ddagger/J \text{ K}^{-1} \text{ mol}^{-1}$
$[\text{PdCl}_2\{\overline{\text{SeCH}_2\text{CMe}_2\text{CH}_2}\}_2]$	82.1	13.4	78.6 ± 0.5	79.2	2.0
$[\text{PdBr}_2\{\overline{\text{SeCH}_2\text{CMe}_2\text{CH}_2}\}_2]$	76.1	12.8	76.0 ± 0.5	73.2	-9.3
$[\text{PdI}_2\{\overline{\text{SeCH}_2\text{CMe}_2\text{CH}_2}\}_2]$	67.8	12.2	71.3 ± 0.5	65.0	-21.4
$[\text{PdCl}_2\{\overline{\text{Se}(\text{CH}_2)_4}\}_2]$	66.6	11.8	72.1 ± 1.2	63.6	-28.7
$[\text{PdBr}_2\{\overline{\text{Se}(\text{CH}_2)_4}\}_2]$	67.6	12.1	71.7 ± 1.2	64.8	-23.1
$[\text{PdI}_2\{\overline{\text{Se}(\text{CH}_2)_4}\}_2]$	58.9	11.6	66.5 ± 1.2	56.2	-26.5
$[\text{PdCl}_2\{\overline{\text{Se}(\text{CH}_2)_5}\}_2]$	71.4	12.7	71.8 ± 0.2	68.5	-11.0
$[\text{PdBr}_2\{\overline{\text{Se}(\text{CH}_2)_5}\}_2]$	67.9	12.3	70.6 ± 0.2	65.0	-18.8
$[\text{PdI}_2\{\overline{\text{Se}(\text{CH}_2)_5}\}_2]$	62.5	12.0	66.7 ± 0.2	59.8	-23.2

* All ΔG^\ddagger data refer to 298.15 K.**Table 7.** Relationship between ground-state geometries and pyramidal inversion barriers^a

Complex	Inverting atom E	Ground-state C-E-C angle (°)	$\Delta G^\ddagger/\text{kJ mol}^{-1}$	Ref.
<i>trans</i> - $[\text{PdCl}_2\{\overline{\text{SeCH}_2\text{CMe}_2\text{CH}_2}\}_2]$	Se	90	78.6	<i>b</i>
<i>trans</i> - $[\text{PdCl}_2\{\overline{\text{Se}(\text{CH}_2)_4}\}_2]$	Se	108	72.1	<i>b</i>
<i>trans</i> - $[\text{PdCl}_2\{\overline{\text{Se}(\text{CH}_2)_5}\}_2]$	Se	108	71.8	<i>b</i>
<i>trans</i> - $[\text{PdCl}_2\{\overline{\text{Se}(\text{CH}_2\text{SiMe}_3)_2}\}_2]$	Se	108 ^c	69.3	20
<i>trans</i> - $[\text{PdCl}_2\{\overline{\text{SCMe}_2\text{CMe}_2}\}_2]$	S	60	>90	2
<i>trans</i> - $[\text{PdCl}_2\{\overline{\text{SCH}_2\text{CMe}_2\text{CH}_2}\}_2]$	S	90	60.9	2
<i>trans</i> - $[\text{PdCl}_2\{\overline{\text{S}(\text{CH}_2)_4}\}_2]$	S	108	56.1	2
<i>trans</i> - $[\text{PdCl}_2\{\overline{\text{S}(\text{CH}_2)_5}\}_2]$	S	108	55.7	2
<i>trans</i> - $[\text{PdCl}_2\{\overline{(\text{SCH}_2\text{SiMe}_3)_2}\}_2]$	S	108 ^c	54.6	20
$\text{MeN}(\overline{\text{CH}_2})_3$	N	90	37.9 ^d	<i>e</i>
$\text{MeN}(\overline{\text{CH}_2})_4$	N	108	30.3 ^d	<i>e</i>

^a All ΔG^\ddagger data refer to 298.15 K. ^b Present work. ^c Open-chain ligands. ^d Literature values at coalescence temperatures converted to 298.15 K. ^e J. B. Lambert, W. L. Oliver, and B. S. Packard, *J. Am. Chem. Soc.*, 1971, **93**, 933.

selenium inversion is slow and there is a very small geminal internal chemical shift. In either case, the splitting is primarily due to vicinal coupling ($^3J \approx 6$ Hz). Warming the complex in $\text{C}_6\text{D}_5\text{NO}_2$ solution to *ca.* 120 °C and cooling in CD_2Cl_2 solution to *ca.* 90 °C revealed only very slight changes in the spectra. The α -methylene triplet changed from a sharp signal at above-ambient temperature to a less well-defined triplet at low temperatures. This latter spectral change is thought to be due to the freezing out of selenium inversion. The chloro- and bromo-complexes produced similar spectra to the iodo-complex but at somewhat different temperatures. For example, solutions of these complexes required warming in order to produce the pseudo-triplet appearance of the α -methylene band. This implies that the selenium inversion process was somewhat less facile in these complexes compared to the iodo-complex. On account of these very slight and ill defined spectral changes, it was not possible to perform any dynamic n.m.r. bandshape analyses. Very high field studies (*viz.* 400-MHz ^1H spectra) would be essential for any quantitative study of inversion in these complexes, and such facilities were not available at the time.

Discussion

The static parameters of the α -methylene protons of the complexes, given in Tables 2 and 3, show that the geminal distinction of the protons as a result of slow selenium inversion varies between 0.4 and 1.1 p.p.m. The deshielding by the PdX_2 moiety on the SeCH_2 protons affects the A,A' protons more

strongly than the B,B' protons by virtue of their closer proximity to the PdX_2 group. The shifts are also consistently dependent on halogen such that an increase in halogen size causes higher frequency shifts. An analogous trend was noted for the ring sulphide complexes.²

The Arrhenius and Eyring energy parameters for selenium inversion in the three-, four-, and five-membered ring selenide complexes are collected in Table 6.

Variation in Ligand Ring Size.—Comparison of free energies of activation for the same halogen complexes of different ligand ring size shows a consistent trend to lower energies as the ring size increases. For example, for the chloro-complexes $[\text{PdCl}_2\{\overline{\text{SeCH}_2\text{CMe}_2\text{CH}_2}\}_2]$, $[\text{PdCl}_2\{\overline{\text{Se}(\text{CH}_2)_4}\}_2]$, and $[\text{PdCl}_2\{\overline{\text{Se}(\text{CH}_2)_5}\}_2]$, ΔG^\ddagger values are 78.6, 72.1, and 71.8 kJ mol^{-1} respectively. Comparable trends were observed in the ring sulphide complexes,² the sulphur inversion barriers being 15–20 kJ mol^{-1} lower in absolute magnitudes compared to the selenium barriers.

The energy of the pyramidal inversion process is a function of the ease whereby the pyramidal atom E achieves a trigonal-planar transition state with a C-E-C angle of 120°. Whereas in acyclic ligands this may be achieved without any significant angle strain, if the inverting atom is a ring heteroatom its ease of attaining the transition state is reduced. This angle strain factor varies considerably with ligand ring size as illustrated in Table 7. It is particularly important for three- and four-

membered rings, as reflected in the particularly high ΔG^\ddagger values for inversion in these cyclic ligand complexes. Five-, six-, and seven-membered rings are much more able to accommodate the geometric changes required to achieve the transition state structures, and their ΔG^\ddagger data for chalcogen inversion are fairly insensitive to ring size. No data were calculable for the seven-membered selenepane complexes but qualitative estimates imply energies slightly lower than the six-membered ring complexes and comparable to those of acyclic selenoether complexes as exemplified by the complexes $[\text{PdCl}_2\{\text{Se}(\text{CH}_2\text{CH}_3)_2\}_2]$ ¹⁹ and $[\text{PdCl}_2\{\text{Se}(\text{CH}_2\text{SiMe}_3)_2\}_2]$.²⁰

Variation in Halogen.—Another feature of the data in Table 6 is the consistent decrease of selenium inversion energies with halogen in the order $\text{Cl} > \text{Br} > \text{I}$. This decrease in ΔG^\ddagger values is greater than 7 kJ mol^{-1} for the four-membered ring complexes and therefore represents a very significant *cis* halogen influence. *trans* Halogen influences are widely known²¹ and have been observed for sulphur inversion in *cis* complexes such as *cis*- $[\text{MX}_2\text{L}']$ ($\text{M} = \text{Pd}$ or Pt , $\text{X} = \text{halogen}$, $\text{L}' = \text{MeSCH}_2\text{CH}_2\text{-SMe}$).²² However, *cis* halogen influences are far less common although they were clearly in evidence in the analogous ring sulphide complexes of palladium(II) and platinum(II).² The effect decreases as the ring size increases suggesting an electronic rather than steric explanation. It has been noted that increasing the electronegativity of substituents attached to an inverting centre correlates well with an increase in inversion energy.^{23,24} This can be explained in terms of slight contractions of the metal *d* orbitals under the influence of electronegative substituents, thus reducing the (*p-d*) π contribution to the stabilisation of the inversion transition state. Such reasoning can be applied to the present complexes, whereby an increase in the electronegativity of the PdX_2 moiety effectively reduces the stabilisation of the planar selenium atom transition state.

Acknowledgements

We thank Dr. Martin Smith (Brüker Spectrospin Ltd., Canada) for the 63-MHz ¹³C spectrum of $[\text{PdCl}_2\{\text{Se}(\text{CH}_2)_5\}_2]$, and Dr. Janos Mink for i.r. and Raman measurements.

References

- 1 E. W. Abel, S. K. Bhargava, and K. G. Orrell, *Prog. Inorg. Chem.*, 1984, **32**, 1.
- 2 E. W. Abel, M. Booth, and K. G. Orrell, *J. Chem. Soc., Dalton Trans.*, 1979, 1994.
- 3 E. W. Abel, M. Booth, and K. G. Orrell, *J. Chem. Soc., Dalton Trans.*, 1980, 1582.
- 4 A. B. Callear and W. J. R. Tyerman, *Proc. Chem. Soc.*, 1964, 296.
- 5 G. H. Schmid and D. G. Garratt, *Tetrahedron Lett.*, 1975, 3991.
- 6 G. T. Morgan and F. H. Burstall, *J. Chem. Soc.*, 1929, 1096.
- 7 G. T. Morgan and F. H. Burstall, *J. Chem. Soc.*, 1929, 2197.
- 8 J. D. McCullough and A. Lefohn, *Inorg. Chem.*, 1966, **5**, 150.
- 9 G. T. Morgan and F. H. Burstall, *J. Chem. Soc.*, 1931, 173.
- 10 H. J. Backer and H. J. Winter, *Recl. Trav. Chim. Pay-Bas*, 1937, **56**, 492.
- 11 (a) D. A. Kleier and G. Binsch, DNMR3, Program 165, Quantum Chemistry Program Exchange, Indiana University, U.S.A., 1970; (b) A. A. Bothner-By and S. Castellano, *J. Chem. Phys.*, 1964, **41**, 3863; (c) D. F. Detar, 'Computer Programs for Chemistry,' W. A. Benjamin, 1968, vol. 1.
- 12 G. T. Morgan and F. H. Burstall, *J. Chem. Soc.*, 1930, 1497.
- 13 M. G. Petit, J. S. Gibson, and D. O. Harris, *J. Chem. Phys.*, 1970, **53**, 3408.
- 14 W. H. Green, A. B. Harvey, and J. A. Greenhouse, *J. Chem. Phys.*, 1971, **54**, 850.
- 15 A. L. Esteban and E. Diez, *J. Magn. Reson.*, 1970, **36**, 113.
- 16 J. B. Lambert and S. I. Featherman, *Chem. Rev.*, 1975, **75**, 611.
- 17 M. Karplus, *J. Chem. Phys.*, 1959, **30**, 11.
- 18 J. B. Hendrickson, *J. Am. Chem. Soc.*, 1962, **84**, 3355; *Tetrahedron*, 1963, **19**, 1387.
- 19 R. J. Cross, T. H. Green, and R. Keat, *J. Chem. Soc., Dalton Trans.*, 1976, 1150.
- 20 E. W. Abel, A. R. Khan, K. Kite, K. G. Orrell, and V. Šik, *J. Chem. Soc., Dalton Trans.*, 1977, 42.
- 21 T. G. Appleton, H. C. Clark, and L. E. Manzer, *Coord. Chem. Rev.*, 1973, **10**, 335.
- 22 E. W. Abel, S. K. Bhargava, K. Kite, K. G. Orrell, V. Šik, and B. L. Williams, *Polyhedron*, 1982, **1**, 289.
- 23 R. D. Baechler and K. Mislow, *J. Am. Chem. Soc.*, 1970, **92**, 4758.
- 24 R. D. Baechler and K. Mislow, *J. Am. Chem. Soc.*, 1971, **93**, 773.

Received 29th April 1985; Paper 5/694